International Journal of Dynamics and Control (2024) 12:382–395
https://doi.org/10.1007/s40435-023-01215-4

Synchronization of complex networks with dynamic parameters uncertainty and mixed delays coupling

Heshan Lei[1] · **Nuo Jia**[1]

Received: 10 January 2023 / Revised: 15 February 2023 / Accepted: 1 May 2023 / Published online: 16 May 2023

Abstract
A new model of projective synchronization and finite-time synchronization for a class of complex networks with dynamic parameters and mixed delays is studied. Time-varying nodal delays, coupling delays and distributed delays are added to the dynamic equations of the model in order to study how the mixed delay affects the dynamic behavior of the network, and the uncertainty of dynamic parameters is also considered in the process of establishing the model, which is more consistent with the actual system and extends its application. After that, a mixed control strategy is proposed to realize outer projective synchronization as well as a newer and simpler controller is proposed to realize finite-time synchronization, both the sufficient condition of the synchronization are given. The stability of the outer projective synchronization and finite-time synchronization are also proved based on Lyapunov stability principle. Finally, numerical simulations are carried out to verify the validity of the obtained theoretical results.

Keywords Complex networks · Outer projective synchronization · Finite-time synchronization · Unknown parameters · Mixed delays · Mixed control strategy

1 Introduction

Nowadays, complex networks have become a subject in many different fields. With the continuous progress of the times, the theoretical achievements of complex networks are remarkable.[1–4] Its earliest theoretical research can be traced back to the "Seven Bridges Problem" in the 18th century, that is, the land is abstracted as a point, and the bridge of continuous land is abstracted as an edge to form a network.[5] In recent years, complex networks with high-dimensional or dynamic nodes of high-dimensional systems have attracted more and more researchers' interest due to their potential applications in physics, chemistry, aerospace and other fields.[6–8] As a result, exploring complex networks has become an important subject today.

Under random initial conditions, due to the existence of coupling, the nodes in the network may evolve into a global synchronization state, or may eventually stabilize in a partial synchronization state.[9] As a common dynamic behavior of complex networks, synchronization has been studied by many scholars, such as lag synchronization,[10] cluster synchronization,[11] projective synchronization,[12] exponential synchronization,[13]. The common methods of network synchronization control include adaptive control, traction control, intermittent control,[14] etc. Projective synchronization is one of the important styles, which refers to a state in which the drive network and the response network can maintain synchronization under a scale factor difference, that is, when the scale factor is 1, the synchronization between such two networks is called complete synchronization.[15] Its accuracy lies in the mixture of projective synchronization and scale factor, which deepens the complexity of synchronization and plays an important role in secure transmission.[16] In recent years, as an important synchronization way, projective synchronization has been widely used for complex networks. For example, in [17] an adaptive synchronization controller is designed to achieve modified function projective synchronization between presented complex networks with known or unknown parameters, which consists of a vector function with dynamic behavior and nodes with an internal coupling matrix. In [18], taking the projective synchroniza-

✉ Heshan Lei
heshan961@outlook.com

Nuo Jia
anuo1978@126.com

[1] Department of Mathematics, Harbin Normal University, Division Road, Harbin 15000, Heilongjiang, China

tion of Lorenz chaotic system and Rössler chaotic system as an example, the pole placement method is used to design the controller which has the advantages of simplicity and faster synchronization speed, the projective synchronization of two chaotic systems is realized. Asymptotic time synchronization refers to the behavior that the states of all nodes in the network tend to be consistent with time. Based on its limitations, finite-time synchronization is proposed.[19] Finite-time synchronization represents a concept of time limits. In [20], for the stochastic complex networks with time delays, an adaptive control method is used to achieve finite-time synchronization between networks with the same structures and different structures. In [21], for complex networks with time-varying nodal delays and mixed coupling, a simple discontinuous state feedback controller is used to achieve finite-time synchronization between generalized complex networks. In [22], the finite-time synchronization problem of MNNs with mixed delays is proposed. In this paper, a new method is used for the first time to study the finite-time synchronization problem of this network model, and a very simple sign function controller is applied to solve this problem.

Both networks and systems are affected by human control or environmental factors, thus interfering with the control effect of network or system synchronization. In real life, unknown parameter interference is a common phenomenon. In [23], the complete synchronization of two complex systems with uncertain parameters, coupled structure and interference are considered and the synchronization condition is pointed out. In nature, the future development trend of the systems may be jointly determined by the past state and the current state, [24] so time-delay is one of the inevitable phenomena in the networks. It can be divided into discrete time delay, distributed time delay, and mixed time delay.[25] The application of time-delay systems is also widespread in real life. In [26], a sliding mode predictive control for the fast tracking problem of pure time-delay system was explored. In [27], a vehicle-following complex networks model with optimal speed and time-varying delay under random disturbances was considered and congestion of road vehicle is alleviated by the stability control of this model. In [28], a stochastic competitive system with a time-varying delay was discussed by applying appropriate functionals and the theory of neutral equilibrium differential equations, the probability of the stability of this type of model in an equilibrium state was solved. These references fully demonstrate the importance of time-varying delays.

As mentioned above, dynamical system uncertainty and time delay are two essential factors to be considered in the synchronization of complex networks. Motivated by these points, a more general complex network model combining the uncertainty of dynamic parameters with the common mixed delays such as nodal delay, coupling delay and distributed delay is given and discussed, which makes the network model more realistic. Compared with the reference [17], our network does not need to meet the Lipschitz condition, and by constructing a mixed nonlinear control strategy with adaptive law, it can achieve projective synchronization. So our results will be more general. Compared with the reference [21], the model we consider is more general and we apply the new method in [22] to simply deal with the finite-time synchronization problem. To sum up, in comparison with the relevant results, the main contributions of this article are listed as follows.

∗ The models used in this paper are new network models that have never appeared before. We fully consider the influence of nodes, coupling structure and distribution state with or without time delays.

∗ Dynamic parameters uncertainty and mixed delays are considered into the time-delay complex network model, which makes our model more versatile.

∗ The article constructed model itself is used for numerical simulation to make the stability of the model more easily verified and the model is applied to secure communication to show that the theory we adopt can deal with general practical problems.

The main structure of this paper is as follows. In Sect. 2, some preliminaries and model descriptions are introduced. The main methods and proofs are given in Sect. 3. In Sect. 4, we verify the feasibility of the synchronization under mixed control strategy and controller by both theoretical proof and numerical simulations. Then, Sect. 5 is an application to secure communication. Finally, Sect. 6 is the conclusion of the paper.

2 Preliminaries and Model Descriptions

Throughout this article, let $\mathbb{I} = \{1, 2, \ldots, N\}$, $\mathbb{R}^q$ and $\mathbb{R}^{N\times N}$ represent the q-dimensional and $N \times N$ dimensional Euclidean spaces respectively. The superscript " -1" represents the inverse of a matrix or vector and also the superscript "T" stands for the transpose of a vector or a matrix. $\|\cdot\|$ represents the Euclidean vector norm.

According to the theory of network dynamics, the state of each node in the network can be described by a dynamic equation $\dot{x_i}(t) = F(x_i(t))$. Consider a linear coupling complex network with nodal delay, coupling delay and distributed delay, and take this network as a drive network. Its state equation is described as

$$\dot{x_i}(t) = F(x_i(t)) + f_1(x_i(t-\tau_0(t))) + \sum_{j=1}^{N} b_{ij} H_1 x_j(t) + \sum_{j=1}^{N} l_{ij} H_2 x_j(t-\tau_1(t)) + \sum_{j=1}^{N} d_{ij} \int_{t-\tau_2(t)}^{t} H_3 x_j(\xi) d\xi \tag{1}$$

where $i \in \mathbb{I}$; $x_i(t) = (x_{i1}(t), x_{i2}(t), \ldots, x_{iq}(t))^T \in \mathbb{R}^q$ represents the state vector of the ith node at time t. The vector function $F(\cdot)$: $\mathbb{R}^q \to \mathbb{R}^q$ drives the network with unknown parameters, and it is guaranteed to be continuous. $H_1(\cdot), H_2(\cdot), H_3(\cdot) : \mathbb{R}^{q\times q} \to \mathbb{R}^{q\times q}$ are the internal coupling matrices in the drive network. The vector function $f_1 : \mathbb{R}^q \to \mathbb{R}^q$ is a nonlinear smooth function, and it represents the dynamic characteristics of the network. $\tau_0(t) \geq 0$ is the time-varying delay of the node, $\tau_1(t) \geq 0$ and $\tau_2(t) \geq 0$ are the coupled time-varying delay, and the distributed delay of the system. The non-delay outer-coupling matrix $B = (b_{ij})_{N\times N} \in \mathbb{R}^{N\times N}$ and the time-delay outer-coupling matrix $L = (l_{ij})_{N\times N} \in \mathbb{R}^{N\times N}$, $D = (d_{ij})_{N\times N} \in \mathbb{R}^{N\times N}$ describe the topology of the networks and they are required to satisfy the following conditions: if there is non-delay coupling between nodes i and j $(i \neq j)$, then $b_{ij} > 0$, otherwise $b_{ij} = 0$. Similarly, if the node i and j $(i \neq j)$are coupled with time delay, then $l_{ij} > 0$, $d_{ij} > 0$, otherwise $l_{ij} = d_{ij} = 0$. In addition, the matrices B, L and D all satisfy the dissipative coupling condition

$$\begin{aligned} b_{ii} &= -\sum_{j=1,j\neq i}^{N} b_{ij} = -\sum_{j=1,j\neq i}^{N} b_{ji}, l_{ii} = -\sum_{j=1,j\neq i}^{N} l_{ij} \\ &= -\sum_{j=1,j\neq i}^{N} l_{ji}, \\ d_{ii} &= -\sum_{j=1,j\neq i}^{N} d_{ij} = -\sum_{j=1,j\neq i}^{N} d_{ji} \end{aligned} \tag{2}$$

where$i \in \mathbb{I}$. Since $F(\cdot)$ is a dynamic function with unknown parameters, we define $F(x_i(t)) = A(x_i(t))\alpha + f(x_i(t))$, where $A : \mathbb{R}^q \to \mathbb{R}^{q\times m}$ and $f : \mathbb{R}^q \to \mathbb{R}^q$ are two functions of the node state vector,$\alpha = (\alpha_1, \alpha_2, \ldots, \alpha_m)^T \in \mathbb{R}^m$ are unknown parameter vectors, and m is the number of unknown parameters. In spite that there is often a certain coupling strength between networks, we default the coupling strength of the time-delay and non-delay parts to be 1 for convenience.

Based on the drive-response concept of synchronization, we give the corresponding response network model

$$\begin{aligned} \dot{y}_i(t) = G(y_i(t)) &+ f_1(y_i(t-\tau_0(t))) + \sum_{j=1}^{N} b_{ij} H_1 y_j(t) \\ &+ \sum_{j=1}^{N} l_{ij} H_2 y_j(t-\tau_1(t)) \\ &+ \sum_{j=1}^{N} d_{ij} \int_{t-\tau_2(t)}^{t} H_3 y_j(\xi) d\xi + u_i(t) \end{aligned} \tag{3}$$

where $i \in \mathbb{I}$;$y_i(t) = (y_{i1}(t), y_{i2}(t), \ldots, y_{iq}(t))^T \in \mathbb{R}^q$ represents the state vector of the ith node at time t. $u_i(t) = (u_{i1}(t), u_{i2}(t), \ldots, u_{iq}(t))^T \in \mathbb{R}^q$ is a control vector function to be designed. According to the state error vector of the nodes between the drive-response network systems, the states of the nodes in the response network are continuously adjusted. The rest of the variables are represented in the same way as the drive network.

The assumptions and related definition and lemmas needed are given below.

Assumption 1 $\tau_i(t)$ is continuously differentiable, satisfying

$$0 < \tau_i(t) < \tau_i, 0 < \dot{\tau}_i(t) < \mu_K < \mu < 1, \quad i \in \mathbb{I}$$

.

Assumption 2 Assume that the network topology matrix D is satisfied the following bounded conditions

$$\sum_{i=1}^{N} (d_{ij})^2 < d, \quad i \in \mathbb{I}$$

Remark 1 The above two assumptions, that is, the time-delay and the conditions that the matrix satisfies, are assumed to ensure the existence of solutions Eqs. (1) and (3) in the corresponding initial conditions. In addition, many systems with time-delay have this condition, and the authors in [22, 23] make a similar assumption. Therefore, the assumptions in this paper are reasonable and necessary.

Definition 1 [29] For any continuously differentiable scale function matrix $M(t)$, if

$$\lim_{t\to\infty} \|e_i(t)\| = \lim_{t\to\infty} \|y_i(t) - M(t)x_i(t)\| = 0 \tag{4}$$

then it is called projective synchronization between the n-dimensional drive network and the m-dimensional response network. Here each line element of the function matrix $M(t) = (m_{ij}(t)) \in \mathbb{R}^{m\times n}$ cannot be 0 at the same time, $e_i(t)$ is the error between the state variables of two network nodes.

Lemma 1 [30] *For any positive definite symmetric matrix $Q \in R^{n\times n}$ and $x, y \in R^n$, then*

$$\pm 2x^T y \leq x^T Q x + y^T Q^{-1} y.$$

Lemma 2 [31] *For the vector function $\gamma(t) : [a, b] \to \mathbb{R}^n$, it has*

$$(\int_a^b \gamma(t)dt)^T W \int_a^b \gamma(t)dt \leq (b-a)\int_a^b \gamma^T(t) W \gamma(t) dt$$

for any symmetric positive definite matrix W.

3 Main Results

3.1 Two networks, same structures

In this section, based on the Lyapunov method, a mixed control strategy is presented and the corresponding theoretical criterion is given.

The errors between the state variables of drive-response network nodes are defined as follows

$$e_i(t) = [e_{i1}(t), e_{i2}(t), \ldots, e_{iq}(t)]^T = y_i(t) - M(t)x_i(t) \quad (5)$$

where $i \in \mathbb{I}$, $M(t) \in \mathbb{R}^{q\times q}$ and the derivative of this error can be obtained by

$$\dot{e}_i(t) = \dot{y}_i(t) - \dot{M}(t)x_i(t) - M(t)\dot{x}_i(t) \quad (6)$$

Tidy up to get

$$\begin{aligned}\dot{e}_i(t) = {} & G(y_i(t)) + f_1(y_i(t-\tau_0(t))) + \sum_{j=1}^{N} b_{ij}H_1 y_j(t) \\ & + \sum_{j=1}^{N} l_{ij}H_2 y_j(t-\tau_1(t)) \\ & + \sum_{j=1}^{N} d_{ij}\int_{t-\tau_2(t)}^{t} H_3 y_j(\xi)d\xi - \dot{M}(t)x_i(t) \\ & - M(t)[A(x_i(t))\alpha + f(x_i(t)) \\ & + f_1(x_i(t-\tau_0(t))) + \sum_{j=1}^{N} b_{ij}H_1 x_j(t) \\ & + \sum_{j=1}^{N} l_{ij}H_2 x_j(t-\tau_1(t)) \\ & + \sum_{j=1}^{N} d_{ij}\int_{t-\tau_2(t)}^{t} H_3 x_j(\xi)d\xi] + u_i(t) \end{aligned} \quad (7)$$

The mixed control strategy made up of nonlinear and adaptive law is given as

$$u_i(t) = u_{i1}(t) + u_{i2}(t) + u_{i3}(t) \quad (8)$$

where

$$\begin{cases} u_{i1}(t) = -G(y_i(t)) + M(t)f(x_i(t)) \\ \qquad + \dot{M}(t)x_i(t) - f_1(y_i(t-\tau_0(t))) \\ \qquad + M(t)f_1(x_i(t-\tau_0(t))) + M(t)A(x_i(t))\hat{\alpha}(t) \\ u_{i2}(t) = \sum_{j=1}^{N}\widetilde{\upsilon}_{ij}^{1}H_1 y_j(t) + \sum_{j=1}^{N}\widetilde{\upsilon}_{ij}^{2}H_2 y_j(t-\tau_1(t)) \\ \qquad + \sum_{j=1}^{N}\widetilde{\upsilon}_{ij}^{3}\int_{t-\tau_2(t)}^{t} H_3 y_j(\xi)d\xi \\ u_{i3}(t) = -E_i(t)e_i(t) \end{cases} \quad (9)$$

which satisfy

$$\begin{cases} \dot{\hat{\alpha}}(t) = \sum_{j=1}^{N} -M(t)A^T(x_i(t))e_i(t) \\ \dot{E}_i(t) = \delta_i e_i^T(t)e_i(t) \\ \dot{\widetilde{\upsilon}}_{ij}^{1} = -e_i^T(t)PH_1 y_j(t) \\ \dot{\widetilde{\upsilon}}_{ij}^{2} = -e_i^T(t)PH_2 y_j(t-\tau_1(t)) \\ \dot{\widetilde{\upsilon}}_{ij}^{3} = -e_i^T(t)P\int_{t-\tau_2(t)}^{t} H_3 y_j(\xi)d\xi \end{cases} \quad (10)$$

Remark 2 Equation (10) in order to satisfy the conditions needed in the application of Lyapunov function in the following.

Here $\delta_i > 0$ is arbitrary constant and $P = diag(p_1, p_2, \ldots, p_q)$ is a positive definite diagonal matrix. Then the following theorem is obtained.

Theorem 1 *For drive system Eq. (1) and response system Eq. (3) under Assumptions 1–2. Assume there is a symmetric positive definite matrix $Q \in \mathbb{R}^{q\times q}$ such that*

$$\begin{aligned} & \lambda_{max}(B \otimes H_1) + d^2\varepsilon\lambda_{max}(I) \\ & + \lambda_{max}(Q) - \lambda_{max}(\Upsilon) + \lambda_{max}(L \otimes H_2) < 0 \\ & \varepsilon^{-1}N - 1 < 0 \end{aligned}$$

where $\lambda_{max}(\cdot)$ denote the maximum eigenvalues, $\bar{d}_i > 0$ is an undetermined sufficiently large positive number and ε also a positive number, $I \in \mathbb{R}^{q\times q}$ is an identity matrix and $\Upsilon = diag(\bar{d}_1, \bar{d}_2, \ldots, \bar{d}_q)$, then the drive-response systems achieve projective synchronization under the mixed control strategy Eq. (9) with adaptive law Eq. (10).

Proof Choose the following Lyapunov function

$$\begin{aligned} V(t) = {} & \frac{1}{2}\sum_{i=1}^{N} e_i^T(t)Pe_i(t) + \frac{1}{2}\sum_{i=1}^{N}\tilde{\alpha}_i^T(t)P\tilde{\alpha}_i(t) \\ & + \sum_{i=1}^{N} p_i\int_{t-\tau_1(t)}^{t}\tilde{e}_i^T(\theta)Q\tilde{e}_i(\theta)d\theta \\ & + \frac{1}{2}\sum_{i=1}^{N}\sum_{j=1}^{N}(2b_{ij} + \widetilde{\upsilon}_{ij}^{1})^2 + \frac{1}{2}\sum_{i=1}^{N}\sum_{j=1}^{N}(2l_{ij} + \widetilde{\upsilon}_{ij}^{2})^2 \\ & + \frac{1}{2}\sum_{i=1}^{N}\sum_{j=1}^{N}(3d_{ij} + \widetilde{\upsilon}_{ij}^{3})^2 \\ & + \tau_2\sum_{i=1}^{N}\int_{-\tau_2}^{t}d\theta\int_{\theta+t}^{\theta}[e_i^T(\xi)H_3^T H_3 e_i(\xi)]d\xi \\ & + \frac{1}{2}\sum_{i=1}^{N}\frac{1}{\delta_i}(E_i(t) - \bar{d}_i)^2 \end{aligned} \quad (11)$$

where:

$$
\begin{aligned}
&e_i(t) = (e_{i1}(t), e_{i2}(t), \ldots, e_{iq}(t))^T \\
&\tilde{e}_i(t) = (e_{1i}(t), e_{2i}(t), \ldots, e_{qi}(t))^T \\
&\tilde{\alpha}_i(t) = (\alpha_{i1}(t), \alpha_{i2}(t), \ldots, \alpha_{im}(t))^T \\
&\tilde{\alpha}_i(t) = \hat{\alpha}_i(t) - \alpha_i(t)
\end{aligned} \tag{12}
$$

the derivation along the error system can be calculated as follows

$$
\begin{aligned}
\dot{V}(t) = &\sum_{i=1}^{N} e_i^T(t) P \dot{e}_i(t) + \sum_{i=1}^{N} \tilde{\alpha}_i^T(t) \dot{\tilde{\alpha}}_i(t) + \sum_{i=1}^{N} p_i \tilde{e}_i^T(t) Q \tilde{e}_i(t) \\
&- \sum_{i=1}^{N} p_i (1-\mu) \tilde{e}_i{}^T(t-\tau_1(t)) Q \tilde{e}_i(t-\tau_1(t)) \\
&+ \sum_{i=1}^{N} \sum_{j=1}^{N} (2b_{ij} + \widetilde{\upsilon_{ij}^1}) \cdot \dot{\widetilde{\upsilon_{ij}^1}} \\
&+ \sum_{i=1}^{N} \sum_{j=1}^{N} (2l_{ij} + \widetilde{\upsilon_{ij}^2}) \cdot \dot{\widetilde{\upsilon_{ij}^2}} + \sum_{i=1}^{N} \sum_{j=1}^{N} (3d_{ij} + \widetilde{\upsilon_{ij}^3}) \cdot \dot{\widetilde{\upsilon_{ij}^3}} \\
&- \tau_2 \sum_{i=1}^{N} \int_{t-\tau_2(t)}^{t} e_i^T(\xi) H_3^T H_3 e_i(\xi) d\xi \\
&+ \sum_{i=1}^{N} (E_i(t) - \bar{d}_i) \cdot \dot{E}_i(t)
\end{aligned} \tag{13}
$$

Here

$$
\begin{aligned}
\sum_{i=1}^{N} e_i^T(t) P \dot{e}_i(t) = &\sum_{i=1}^{N} e_i^T(t) P [G(y_i(t)) + f_1(y_i(t-\tau_0(t)))] \\
&+ \sum_{j=1}^{N} b_{ij} H_1 y_j(t) + \sum_{j=1}^{N} l_{ij} H_2 y_j(t-\tau_1(t)) \\
&+ \sum_{j=1}^{N} d_{ij} \int_{t-\tau_2(t)}^{t} H_3 y_j(\xi) d\xi \\
&- \dot{M}(t) x_i(t) - M(t)(A(x_i(t))\alpha + f(x_i(t)) \\
&+ f_1(x_i(t-\tau_0(t))) \\
&+ \sum_{j=1}^{N} b_{ij} H_1 x_j(t) + \sum_{j=1}^{N} l_{ij} H_2 x_j(t-\tau_1(t)) \\
&+ \sum_{j=1}^{N} d_{ij} \int_{t-\tau_2(t)}^{t} H_3 x_j(\xi) d\xi) + u_i(t)]
\end{aligned} \tag{14}
$$

Combine together under assumption 1–2 to get

$$
\begin{aligned}
\dot{V}(t) = &\sum_{i=1}^{N} e_i^T(t) P [G(y_i(t)) + f_1(y_i(t-\tau_0(t)))] \\
&+ \sum_{j=1}^{N} b_{ij} H_1 y_j(t) + \sum_{j=1}^{N} l_{ij} H_2 y_j(t-\tau_1(t)) \\
&+ \sum_{j=1}^{N} d_{ij} \int_{t-\tau_2(t)}^{t} H_3 y_j(\xi) d\xi - \dot{M}(t) x_i(t) \\
&- M(t)(A(x_i(t))\alpha + f(x_i(t)) + f_1(x_i(t-\tau_0(t))) \\
&+ \sum_{j=1}^{N} b_{ij} H_1 x_j(t) + \sum_{j=1}^{N} l_{ij} H_2 x_j(t-\tau_1(t)) \\
&+ \sum_{j=1}^{N} d_{ij} \int_{t-\tau_2(t)}^{t} H_3 x_j(\xi) d\xi) + u_i(t)] \\
&+ \sum_{i=1}^{N} \tilde{\alpha}_i{}^T P (- \sum_{i=1}^{N} M(t) A^T(x_i(t)) e_i(t)) \\
&+ \sum_{i=1}^{N} p_i \tilde{e}_i(t) Q \tilde{e}_i(t) \\
&- \sum_{i=1}^{N} p_i (1-\mu) \tilde{e}_i{}^T(t-\tau_1(t)) Q \tilde{e}_i(t-\tau_1(t)) \\
&+ \sum_{i=1}^{N} \sum_{j=1}^{N} (2b_{ij} + \widetilde{\upsilon_{ij}^1}) \cdot [-e_i^T(t) P H_1 y_j(t)] \\
&+ \sum_{i=1}^{N} \sum_{j=1}^{N} (2l_{ij} + \widetilde{\upsilon_{ij}^2}) \cdot [-e_i^T(t) P H_2 y_j(t-\tau_1(t))] \\
&+ \sum_{i=1}^{N} \sum_{j=1}^{N} (3d_{ij} + \widetilde{\upsilon_{ij}^3}) \cdot [-e_i^T(t) P \int_{t-\tau_2(t)}^{t} H_3 y_j(\xi) d\xi] \\
&- \tau_2 \sum_{i=1}^{N} \int_{t-\tau_2(t)}^{t} e_i^T(\xi) H_3^T H_3 e_i(\xi) d\xi \\
&+ \sum_{i=1}^{N} (E_i(t) - \bar{d}_i) \cdot e_i(t)^T e_i(t)
\end{aligned} \tag{15}
$$

According to Lemmas 1 and 2 we have

$$
\begin{aligned}
\dot{V}(t) \le &\lambda_{max}(B \otimes H_1) \sum_{i=1}^{N} p_i \tilde{e}_i{}^T(t) \tilde{e}_i(t) \\
&+ \lambda_{max}(L \otimes H_2) \sum_{i=1}^{N} p_i \tilde{e}_i{}^T(t) \tilde{e}_i(t-\tau_1(t)) \\
&+ 2 \sum_{i=1}^{N} p_i e_i{}^T(t) \sum_{j=1}^{N} d_{ij} \int_{t-\tau_2(t)}^{t} H_3 e_i(\xi) d\xi \\
&+ \sum_{i=1}^{N} p_i \tilde{e}_i{}^T(t) Q \tilde{e}_i(t) \\
&- \sum_{i=1}^{N} (1-\mu) p_i \tilde{e}_i{}^T(t-\tau_1(t)) Q \tilde{e}_i(t-\tau_1(t)) \\
&- \tau_2 \sum_{i=1}^{N} \int_{t-\tau_2(t)}^{t} e_i^T(\xi) H_3^T H_3 e_i(\xi) d\xi
\end{aligned}
$$

$$-\sum_{i=1}^{N}\bar{d}_i\tilde{e}_i^{\,T}(t)P\tilde{e}_i(t) \tag{16}$$

where the $\otimes$ is the Kronecker product of the matrices and

$$\begin{aligned}
&2\sum_{i=1}^{N} p_i\tilde{e}_i^{\,T}(t)\sum_{j=1}^{N}d_{ij}\int_{t-\tau_2(t)}^{t}H_3e_i(\xi)d\xi\\
&\quad\le 2\sum_{i=1}^{N}\sum_{j=1}^{N}\tilde{e}_i^{\,T}(t)p_id_{ij}\int_{t-\tau_2(t)}^{t}H_3e_i(\xi)d\xi\\
&\quad\le \varepsilon\sum_{i=1}^{N}\sum_{j=1}^{N}\tilde{e}_i^{\,T}(t)p_i(d_{ij})^2p_i\tilde{e}_i(t)\\
&\qquad+\varepsilon^{-1}\sum_{i=1}^{N}\sum_{j=1}^{N}(\int_{t-\tau_2(t)}^{t}H_3e_i(\xi)d\xi)^T\int_{t-\tau_2(t)}^{t}H_3e_i(\xi)d\xi\\
&\quad\le \varepsilon\sum_{i=1}^{N}\sum_{j=1}^{N}\tilde{e}_i^{\,T}(t)p_i(d_{ij})^2p_i\tilde{e}_i(t)\\
&\qquad+\varepsilon^{-1}\sum_{i=1}^{N}\sum_{j=1}^{N}\tau_2\int_{t-\tau_2(t)}^{t}e_i^T(\xi)H_3^TH_3e_i(\xi)d\xi\\
&\quad\le d^2\varepsilon I\sum_{i=1}^{N}p_ie_i^{\,T}(t)\tilde{e}_i^{\,T}(t)+\varepsilon^{-1}N\tau_2\\
&\qquad\sum_{i=1}^{N}\int_{t-\tau_2(t)}^{t}e_i^T(\xi)H_3^TH_3e_i(\xi)d\xi
\end{aligned}\tag{17}$$

sorted it to get

$$\begin{aligned}
\dot{V}(t)\le&\sum_{i=1}^{N}p_i\tilde{e}_i^{\,T}(t)[\lambda_{max}(B\otimes H_1)+d^2\varepsilon\lambda_{max}(I)\\
&+\lambda_{max}(Q)-\lambda_{max}(\Upsilon)]\tilde{e}_i(t)\\
&+\sum_{i=1}^{N}p_i\tilde{e}_i^{\,T}(t(\lambda_{max}(L\otimes H_2)\tilde{e}_i(t-\tau_1(t))\\
&+\sum_{i=1}^{N}p_i\tilde{e}_i^{\,T}(t-\tau_1(t))[-\lambda_{max}(Q)(1-\mu)]\tilde{e}_i(t-\tau_1(t))\\
&+\tau_2(\varepsilon^{-1}N-1)\sum_{i=1}^{N}\int_{t-\tau_2(t)}^{t}e_i^T(\xi)H_3^TH_3e_i(\xi)d\xi
\end{aligned}\tag{18}$$

□

Here obviously $-\lambda_{max}(Q)(1-\mu)<0$. Thus when $\bar{d}_i>0$ is large enough, there is $\lambda_{max}(B\otimes H_1)+d^2\varepsilon\lambda_{max}(I)+\lambda_{max}(Q)-\lambda_{max}(\Upsilon)+\lambda_{max}(L\otimes H_2)<0$. Therefore $\dot{V}(t)<0$ if $\varepsilon^{-1}N-1<0$. According to the Lyapunov stability theory and Barbalat's lemma, when $t\to\infty$, the value of the state error vector $e_i(t)=(e_{i1}(t),e_{i2}(t),\ldots,e_{iq}(t))^T\to 0$. It can be concluded that there is a maximum invariant set $\mathbb{A}=\{e_i=0\,i\in\mathbb{I}\}$ in the set $\mathbb{Z}=\{e_i=0,\Upsilon_i(t)=\bar{d}_i,i\in\mathbb{I}\}$ and the trajectory of the error dynamical system running from any initial value will eventually converge globally to set $\mathbb{Z}$,at the same time that

$$\lim_{t\to\infty}\|y_i(t)-M(t)x_i(t)\|=0$$

It means that the drive system Eq.(1) and the response system Eq.(3) realize the outer projective synchronization.

3.2 Two networks, different structures

In this section, we change the model a little. Consider a complex network for the drive network with different structures which is described as

$$\begin{aligned}
\dot{x}_i(t)=&F(x_i(t))+f_1(x_i(t-\tau_0(t)))+\sum_{j=1}^{N}b_{ij}^{(1)}h_j(x_j(t))\\
&+\sum_{j=1}^{N}l_{ij}^{(1)}h_j(x_j(t-\tau_1(t)))\\
&+\sum_{j=1}^{N}d_{ij}^{(1)}\int_{t-\tau_2(t)}^{t}h_j(x_j(s))ds
\end{aligned}\tag{19}$$

and the corresponding node dynamic equation for the response network model

$$\begin{aligned}
\dot{y}_i(t)=&G(y_i(t))+f_1(y_i(t-\tau_0(t)))+\sum_{j=1}^{N}b_{ij}^{(2)}h_j(y_j(t))\\
&+\sum_{j=1}^{N}l_{ij}^{(2)}h_j(y_j(t-\tau_1(t)))\\
&+\sum_{j=1}^{N}d_{ij}^{(2)}\int_{t-\tau_2(t)}^{t}h_j(y_j(s))ds+u_i(t)
\end{aligned}\tag{20}$$

At this point, the networks have different structures. $h_j(\cdot)\in\mathbb{R}^q$ is a smooth nonlinear function. The initial value of network Eq. (19) is described as $\phi(s)=(\phi_1(s),\phi_2(s),\ldots,\phi_q(s))^T\in C([-\tau,0],\mathbb{R}^q)$, where $\tau=max\{\tau_0,\tau_1,\tau_2\}$. The same that the initial value of network Eq. (20) such $\varphi(s)=(\varphi_1(s),\varphi_2(s),\ldots,\varphi_q(s)^T\in C([-\tau,0],\mathbb{R}^q)$. The other representations are the same as the above models. Here we need to add the following assumption and definition.

Assumption 3 For $\forall x,y\in R$ there exist constants $\zeta_i>0,i\in\mathbb{I}$, such that

$$|\,h_i(y)-h_i(x)\,|\le\zeta_i\,|\,y-x\,|$$

Remark 3 The same under the assumption 3, there exist constants $\xi_i, \omega > 0$, such that $| h_i(x) | \leq \xi_i, | f_1(x) - f_1(y) | \leq \omega | x - y |$. That is to say that ensure the nonlinear function is continuous and bounded. In this way, the existence of the solution satisfies the networks.

Definition 2 The drive system Eq. (19) is be synchronized with the response system Eq. (20) in finite-time, if there exist constant $t^* > 0$, such that

$$\lim_{t\to t^*} \|e_i(t)\| = \lim_{t\to t^*} \|y_i(t) - x_i(t)\| = 0, \quad t > t^*$$

The errors between the state variables of drive-response network nodes are defined as follows

$$e_i(t) = y_i(t) - x_i(t), \quad i \in \mathbb{I} \tag{21}$$

and the derivative of this error can be obtained by

$$\dot{e}_i(t) = \dot{y}_i(t) - \dot{x}_i(t) \tag{22}$$

Tidy up to get

$$\begin{aligned}\dot{e}_i(t) = {} & G(y_i(t)) - A(x_i(t))\alpha(t) - f(x_i(t)) \\ & + f_1(e_i(t-\tau_0(t))) + \sum_{j=1}^{N} b_{ij}^{(1)} g_j(e_j(t)) \\ & + \sum_{j=1}^{N} l_{ij}^{(1)} g_j(e_j(t-\tau_1(t))) \\ & + \sum_{j=1}^{N} d_{ij}^{(1)} \int_{t-\tau_2(t)}^{t} g_j(e_j(s))ds \\ & + \sum_{j=1}^{N} (b_{ij}^{(2)} - b_{ij}^{(1)}) h_j(y_j(t)) \\ & + \sum_{j=1}^{N} (l_{ij}^{(2)} - l_{ij}^{(1)}) h_j(y_j(t-\tau_1(t))) \\ & + \sum_{j=1}^{N} (d_{ij}^{(2)} - d_{ij}^{(1)}) \int_{t-\tau_2(t)}^{t} h_j(y_j(s))ds + u_i(t)\end{aligned} \tag{23}$$

where $g_j(e_j(\cdot)) = h_j(y_j(\cdot)) - h_j(x_j(\cdot)), j \in \mathbb{I}$. Select the feedback controller that with the delay-independent as follows

$$\begin{aligned}u_i(t) = {} & A(x_i(t))\hat{\alpha}(t) + f(x_i(t)) - G(y_i(t)) \\ & -\eta e_i(t) - \varrho sign(e_i(t))\end{aligned} \tag{24}$$

Here $sign(e_i(t)) = (sign(e_1(t)), sign(e_2(t)), \ldots, sign(e_q(t)))^T$, $\tilde{\alpha}(t) = \hat{\alpha}(t) - \alpha(t)(\tilde{\alpha}(t) = 0$,if $t = 0), \dot{\tilde{\alpha}}(t) = \sum_{i=1}^{N} -A^T(x_i(t))\tilde{\alpha}_i(t)$, the normal numbers $\eta, \varrho > 0$ as the control gains.

Theorem 2 *For drive system Eq. (19) and response system Eq. (20) under Assumption 3, if the control gains η and ϱ satisfy*

$$\begin{aligned}\eta \geq {} & \bar{\zeta}(\|\bar{B}\|_1 + \frac{\|\bar{L}\|_1}{1-\mu} + \tau_2\|\bar{D}\|_1) + \frac{\omega}{1-\mu} \\ \varrho > {} & \bar{\xi}(\|B^{(2)} - B^{(1)}\|_\infty + \|L^{(2)} - L^{(1)}\|_\infty \\ & + \tau_2\|D^{(2)} - D^{(1)}\|_\infty)\end{aligned}$$

where $\bar{B} = max\{B^{(1)}, B^{(2)}\}$, $\bar{L} = max\{L^{(1)}, L^{(2)}\}$, $\bar{D} = max\{D^{(1)}, D^{(2)}\}$, $\bar{\zeta} = max\{\zeta_1, \zeta_2, \ldots, \zeta_N\}$, $\bar{\xi} = max\{\xi_1, \xi_2, \ldots, \xi_N\}$. Therefore the drive system Eq. (19) and response system Eq. (20) in finite time synchronization under the controller Eq. (24) and t^* satisfy

$$\begin{aligned}t^* < {} & \frac{1}{\beta}[\|e(0)\|_1 + \frac{\omega}{1-\mu}\int_{-\tau_0(0)}^{0} \|e(s)\|_1 ds \\ & + \frac{\bar{\zeta}}{1-\mu}\|\bar{L}\|_1 \int_{-\tau_1(0)}^{0} \|e(s)\|_1 ds \\ & + \frac{\bar{\zeta}}{1-\mu}\|\bar{D}\|_1 \int_{-\tau_2(0)}^{0}\int_{s}^{0} \|e(w)\|_1 dwds]\end{aligned}$$

where $\beta = \varrho - \bar{\xi}(\|B^{(2)} - B^{(1)}\|_\infty + \|L^{(2)} - L^{(1)}\|_\infty + \tau_2\|D^{(2)} - D^{(1)}\|_\infty)$

Proof Choose the following Lyapunov function

$$\begin{aligned}V(t) = {} & \sum_{i=1}^{N} sign^T(e_i(t))e_i(t) + sign^T(\tilde{\alpha}(t))\tilde{\alpha}(t) \\ & + \sum_{i=1}^{N} \frac{\omega}{1-\mu}\int_{t-\tau_0(t)}^{t} \|e_i(s)\|_1 ds \\ & + \sum_{i=1}^{N} \frac{\bar{\zeta}}{1-\mu}\|\bar{L}\|_1 \int_{t-\tau_1(t)}^{t} \|e_i(s)\|_1 ds \\ & + \sum_{i=1}^{N} \bar{\zeta}\|\bar{D}\|_1 \int_{-\tau_2(t)}^{0}\int_{t+s}^{t} \|e_i(w)\|_1 dwds\end{aligned} \tag{25}$$

the derivation along the error system under the assumption 1 can be calculated as follows

$$\begin{aligned}\dot{V}(t) \leq {} & \sum_{i=1}^{N} sign^T(e_i(t))[G(y_i(t)) - A(x_i(t))\tilde{\alpha}_i(t) \\ & - f(x_i(t)) + f_1(e_i(t-\tau_0(t))) \\ & + \sum_{j=1}^{N} \bar{b}_{ij} g_j(e_j(t)) + \sum_{j=1}^{N} \bar{l}_{ij} g_j(e_j(t-\tau_1(t)))\end{aligned}$$

$$
\begin{aligned}
&+\sum_{j=1}^{N}\bar{d}_{ij}\int_{t-\tau_2(t)}^{t}g_j(e_j(s))ds\\
&+\sum_{j=1}^{N}(b_{ij}^{(2)}-b_{ij}^{(1)})h_j(y_j(t))\\
&+\sum_{j=1}^{N}(l_{ij}^{(2)}-l_{ij}^{(1)})h_j(y_j(t-\tau_1(t)))\\
&+\sum_{j=1}^{N}(d_{ij}^{(2)}-d_{ij}^{(1)})\int_{t-\tau_2(t)}^{t}h_j(y_j(s))ds+u_i(t)]\\
&-\sum_{i=1}^{N}sign^T(\tilde{\alpha}_i(t))A^T(x_i(t))\tilde{\alpha}_i(t)\\
&+\sum_{i=1}^{N}\frac{\omega}{1-\mu}[\|e_i(t)\|_1-(1-\dot{\tau_0}(t))\|e_i(t-\tau_0(t))\|_1]\\
&+\sum_{i=1}^{N}\|\bar{L}\|_1\frac{\bar{\zeta}}{1-\mu}[\|e_i(t)\|_1-(1-\dot{\tau_1}(t))\|e_i(t-\tau_1(t))\|_1]\\
&+\bar{\zeta}\|\bar{D}\|_1\int_{-\tau_2}^{0}\|e_i(t)\|_1ds-\bar{\zeta}\|D^{(1)}\|_1\\
&\times\int_{-\tau_2}^{0}\|e_i(t+s)\|_1ds
\end{aligned}
\tag{26}
$$

According to assumption 3 we had sorted it to get

$$
\begin{aligned}
\dot{V}(t)\le&\sum_{i=1}^{N}sign^T(e_i(t))[\omega\mid(e_i(t-\tau_0))\mid\\
&+\sum_{k=1}^{N}\mid\bar{b}_{ik}\mid\zeta_k\mid e_k(t)\mid+\sum_{k=1}^{N}\mid\bar{l}_{ik}\mid\zeta_k\mid e_k(t-\tau_1(t)))\mid\\
&+\sum_{k=1}^{N}\mid\bar{d}_{ik}\mid\zeta_k\int_{t-\tau_2}^{t}\mid e_k(s)\mid ds\\
&+\sum_{k=1}^{N}\mid b_{ik}^{(2)}-b_{ik}^{(1)}\mid h_k(y_k(t))\\
&+\sum_{k=1}^{N}\mid l_{ik}^{(2)}-l_{ik}^{(1)}\mid h_k(y_k(t-\tau_k))\\
&+\sum_{k=1}^{N}\mid d_{ik}^{(2)}-d_{ik}^{(1)}\mid\int_{t-\tau_2}^{t}h_k(y_k(s))ds\\
&-\eta\mid e_i(t)\mid-\varrho\mid sign(e_i(t))\mid]\\
&+\sum_{i=1}^{N}\frac{\omega}{1-\mu}\|e_i(t)\|_1-\sum_{i=1}^{N}\omega\|e_i(t-\tau_0)\|_1\\
&+\sum_{i=1}^{N}\|\bar{L}\|_1\frac{\bar{\zeta}}{1-\mu}\|e_i(t)\|_1\\
&-\sum_{i=1}^{N}\|\bar{L}\|_1\bar{\zeta}\|e_i(t-\tau_1(t))\|_1+\sum_{i=1}^{N}\tau_2\bar{\zeta}\|\bar{D}\|_1\|e_i(t)\|_1\\
&-\sum_{i=1}^{N}\bar{\zeta}\|\bar{D}\|_1\int_{t-\tau_2}^{t}\|e_i(s)\|_1ds
\end{aligned}
\tag{27}
$$

further collation is obtained

$$
\begin{aligned}
\dot{V}(t)\le&\,\omega\|e(t-\tau_0)\|_1+\bar{\zeta}\|\bar{B}\|_1\|e(t)\|_1+\bar{\zeta}\|\bar{L}\|_1\|e(t-\tau_1)\|_1\\
&+\bar{\zeta}\|\bar{D}\|_1\int_{t-\tau_2}^{t}\|e(s)\|_1ds\\
&+\bar{\xi}\|B^{(2)}-B^{(1)}\|_\infty\sum_{i=1}^{N}\chi_i+\bar{\xi}\|L^{(2)}-L^{(1)}\|_\infty\sum_{i=1}^{N}\chi_i\\
&+\tau_2\bar{\xi}\|D^{(2)}-D^{(1)}\|_\infty\sum_{i=1}^{N}\chi_i-\eta\|e(t)\|_1-\varrho\sum_{i=1}^{N}\chi_i\\
&+\frac{\omega}{1-\mu}\|e(t)\|_1-\omega\|e(t-\tau_0)\|_1\\
&+\|\bar{L}\|_1\frac{\bar{\zeta}}{1-\mu}\|e(t)\|_1-\|\bar{L}\|_1\bar{\zeta}\|e(t-\tau_1)\|_1\\
&+\tau_2\bar{\zeta}\|\bar{D}\|_1\|e(t)\|_1-\bar{\zeta}\|\bar{D}\|_1\int_{t-\tau_2}^{t}\|e(s)\|_1ds
\end{aligned}
\tag{28}
$$

here $\chi_i=0$ if $e_i(t)=0, i\in\mathbb{I}$, otherwise $\chi_i=1$. Therefore,

$$
\begin{aligned}
\dot{V}(t)\le&\,\|e(t)\|_1[\bar{\zeta}(\|\bar{B}\|_1+\|\bar{L}\|_1\frac{1}{1-\mu}\\
&+\tau_2\|\bar{D}\|_1)+\frac{\omega}{1-\mu}-\eta]\\
&-\sum_{i=1}^{N}\chi_i(-\bar{\xi}\|B^{(2)}-B^{(1)}\|_\infty-\bar{\xi}\|L^{(2)}\\
&-L^{(1)}\|_\infty-\tau_2\bar{\xi}\|D^{(2)}-D^{(1)}\|_\infty+\varrho)
\end{aligned}
\tag{29}
$$

We can get the following inequality if theorem 2 is satisfied,

$$
\dot{V}(t)\le-\beta\sum_{i=1}^{N}\chi_i \tag{30}
$$

where $\beta=\varrho-(\bar{\xi}\|B^{(2)}-B^{(1)}\|_\infty+\bar{\xi}\|L^{(2)}-L^{(1)}\|_\infty+\tau_2\bar{\xi}\|D^{(2)}-D^{(1)}\|_\infty)>0$. According in [22], since $V(t)\ge0$ and $\dot{V}(t)\le0$, so there must be a constant $V(0)\ge0$ when $t=0$ as well as $\lim_{t\to+\infty}V(t)=V(0)$ if $V(0)\le V(t),\forall t\ge0$. At that time there must be exist $\epsilon=\beta\triangle t$, $\triangle t$ is a sufficiently small positive constant such that

$$
\begin{aligned}
&\mid V(t)-V(0)\mid=V(t)-V(0)<\epsilon,\\
&\mid V(t)-V(t+\triangle t)\mid=V(t)-V(t+\triangle t)<\epsilon,\ \forall t\ge t'
\end{aligned}
\tag{31}
$$

here $\|e(t')\|_1=0$ and $\|e(t)\|_1=0$

Remark 3 Proof by contradiction: At the first $\|e(t_1)\|_1>0$ and $\|e(t)\|_1>0$ if there exist $t_1>t'$ for $t\in[t_1,t_1+\triangle t]$.

Since $\dot{V}(t) \leq -\beta$, integrating both sides of an inequality at the same time such that

$$V(t_1 + \triangle t) - V(t) \leq -\beta \triangle t = \epsilon$$

This contradicts Eq. (31),that is to say that $\|e(t)\|_1 = 0$. Second,$\|e(t')\|_1 > 0$ if exist sufficiently small positive constant ϵ' such that $\|e(t)\|_1 > 0$ for $t \in [t, t + \epsilon']$, obviously contradicts the formula.

According to definition 2, drive network Eq. (19) and response network Eq. (20) achieve finite time synchronization. Here $t^* = inf\{t > 0 \mid \|e(s)\|_1 = 0, s > t\}$. Due to the effect of time delay, we propose $T = t^* + \tau$. Since $\dot{V}(t) \leq -\beta$ for $\forall t \in (0, t^*)$, integrating this inequality we get

$$V(t^*) - V(0) \leq -\beta t^* \Rightarrow V(t^*) \leq V(0) + \beta t^* \tag{32}$$

Since $\dot{V}(t) \leq 0$ for $\forall t \in (t^*, T^*)$, taking the same approach we get $V(t^*) \geq V(T^*) = 0$, according to [22] we get that $V(0) \geq \beta t^*$, therefore $t^* \leq \frac{V(0)}{\beta}$. □

4 Numerical Example

4.1 Example 1

The corresponding numerical simulations are shown in this section. Consider a complex network model with four nodes, its drive system is as follows

$$\begin{aligned}\dot{x_i}(t) = F(x_i(t)) + f_1(x_i(t - \tau_0(t))) + \sum_{j=1}^{4} b_{ij} H_1 x_j(t) \\ + \sum_{j=1}^{4} l_{ij} H_2 x_j(t - \tau_1(t)) \\ + \sum_{j=1}^{4} d_{ij} \int_{t-\tau_2(t)}^{t} H_3 x_j(\xi) d\xi\end{aligned} \tag{33}$$

where $F(\cdot) = A(\cdot)\hat{\alpha} + f(\cdot)$, $A(\cdot) = 2 \cdot tanh(x_i(\cdot))$, $f(\cdot) = \tanh(x_i(\cdot))$, and take $\hat{\alpha} = (a, b, c, d)^T$ as the vector estimates of unknown parameters, where the nominal values are $a = 1.0, b = 5/8, c = 2.8, d = -0.8$. $f_1(\cdot) = \tanh(x_i(\cdot))$ and

$$H_1 = H_2 = H_3 = Q = \begin{pmatrix} 1 & 0 & 0 & 0 \\ 0 & 1 & 0 & 0 \\ 0 & 0 & 1 & 0 \\ 0 & 0 & 0 & 1 \end{pmatrix}$$

$$B = (b_{ij}) = \begin{pmatrix} \frac{1}{5} & 0 & \frac{2}{5} & \frac{2}{5} \\ \frac{3}{5} & \frac{2}{5} & 0 & \frac{2}{5} \\ \frac{3}{5} & \frac{2}{5} & 0 & \frac{2}{5} \\ \frac{2}{5} & \frac{2}{5} & 0 & \frac{3}{5} \end{pmatrix} \tag{34}$$

Similarly, the matrices L,D are expressed as

$$\begin{aligned} L = (l_{ij}) = \begin{pmatrix} \frac{3}{5} & 0 & \frac{3}{10} & \frac{3}{5} \\ 0 & \frac{3}{5} & \frac{3}{5} & 0 \\ 0 & \frac{3}{5} & \frac{3}{5} & 0 \\ \frac{3}{5} & \frac{9}{10} & \frac{3}{5} & 0 \end{pmatrix} \\ D = (d_{ij}) = \begin{pmatrix} \frac{2}{5} & 0 & \frac{7}{10} & 0 \\ 0 & \frac{1}{2} & \frac{3}{5} & 0 \\ \frac{3}{5} & 0 & 0 & \frac{3}{5} \\ 0 & 0 & \frac{4}{5} & \frac{1}{2} \end{pmatrix} \end{aligned} \tag{35}$$

The coupling delay is $\tau_0(t) = \tau_1(t) = \tau_2(t) = 0.01 + 0.02\sin(t)$ for convenience and $\mu = 0.05$. The response system is

$$\begin{aligned}\dot{y_i}(t) = G(y_i(t)) + f_1(y_i(t - \tau_0(t))) + \sum_{j=1}^{4} b_{ij} H_1 y_j(t) \\ + \sum_{j=1}^{4} l_{ij} H_2 y_j(t - \tau_1(t)) \\ + \sum_{j=1}^{4} d_{ij} \int_{t-\tau_2(t)}^{t} H_3 y_j(\xi) d\xi\end{aligned} \tag{36}$$

where $G(\cdot) = y_i(\cdot), f_1 = \tanh(y_i(\cdot))$. The mixed control strategy of the network can be written as

$$\begin{aligned} u_{i1}(t) = &-tanh((y_i(t))) + M(t)tanh(x_i(t)) + \dot{M}(t)x_i(t) \\ &-tanh(y_i(t - \tau_0(t))) \\ &+M(t)tanh(x_i(t-\tau_0(t))) \\ &+M(t) \cdot 2 \cdot tanh(x_i(t))\hat{\alpha}(t) \\ u_{i2}(t) = &\sum_{j=1}^{4} \widetilde{\upsilon_{ij}^1} H_1 y_j(t) + \sum_{j=1}^{4} \widetilde{\upsilon_{ij}^2} H_2 y_j(t - \tau_1(t)) \\ &+ \sum_{j=1}^{4} \widetilde{\upsilon_{ij}^3} \int_{t-\tau_2(t)}^{t} H_3 y_j(\xi) d\xi \\ u_{i3}(t) = &-E_i(t) e_i(t) \end{aligned} \tag{37}$$

with the adaptive parameter updated law

$$\begin{aligned} \dot{\hat{\alpha}}(t) &= \sum_{j=1}^{4} -M(t) \cdot 2 \cdot tanh(x_i(t)) e_i(t) \\ \dot{E}_i(t) &= \delta_i e_i^T(t) e_i(t) \\ \widetilde{\upsilon_{ij}^1} &= -e_i^T(t) P H_1 y_j(t) \end{aligned}$$

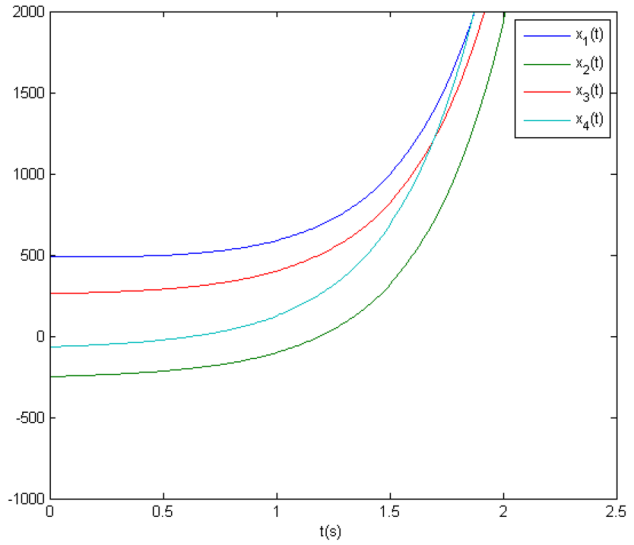

Fig. 1 The trajectories of drive system Eq. (1)

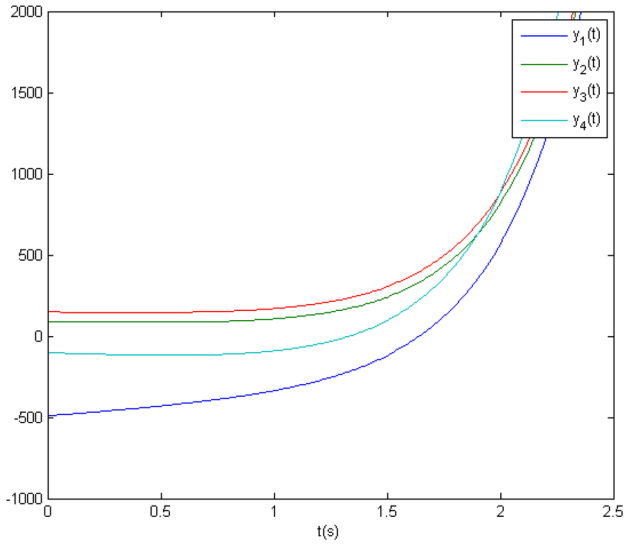

Fig. 2 The trajectories of response system Eq. (3) under control strategy Eq. (9)

$$\begin{aligned}\tilde{\upsilon}_{ij}^{2} &= -e_i^T(t)PH_2y_j(t-\tau_1(t))\\ \tilde{\upsilon}_{ij}^{3} &= -e_i^T(t)P\int_{t-\tau_2(t)}^{t}H_3y_j(\xi)d\xi\end{aligned} \tag{38}$$

The scale function is selected as

$$M(t)=\begin{pmatrix}4+\sin(4t) & 0 & 0 & 0\\ 0 & 2\sin(3t) & 0 & 0\\ 0 & 0 & 0.5+\sin(4t) & 0\\ 0 & 0 & 0 & 3\cos(3t)\end{pmatrix} \tag{39}$$

and the corresponding derivative matrix is

$$\dot{M}(t)=\begin{pmatrix}4\cos(4t) & 0 & 0 & 0\\ 0 & 6\cos(3t) & 0 & 0\\ 0 & 0 & 4\cos(4t) & 0\\ 0 & 0 & 0 & -9\sin(3t)\end{pmatrix} \tag{40}$$

In the above formula, $\delta_i = 2.0$ for $i = 1, 2, \ldots, 4$, $P = diag(1, 1, 1, 1)$. According to [32],we take $\varepsilon = 5$, $d = 0.5$,$\Upsilon = diag(3, 4, 5, 6)$ and by means of calculation, $\lambda_{max}(Q) = \lambda_{max}(I) = 1$,$\lambda_{max}(B \otimes H_1) = 1.2745$, $\lambda_{max}(L \otimes H_2) = 1.2$,. Therefore the conditions required by the Theorem 1 are satisfied

The simulations show that the node dynamic behavior can be affected by the mixed control strategy. Figures 1 and 2 show the motion trajectories of the drive system and the response system. Figure 3 shows the motion trajectory of the error uncontrolled system, and it can be seen that the states are not stable. Figure 4 shows the trajectory of the error system under the mixed control strategy. It is not difficult to see that the 4-dimensional node state error tends to zero and remain steady, which means that the drive system and the response system have achieved the outer projective synchronization of the complex networks after a period of time. So this experiment shows that our theoretical result is valid.

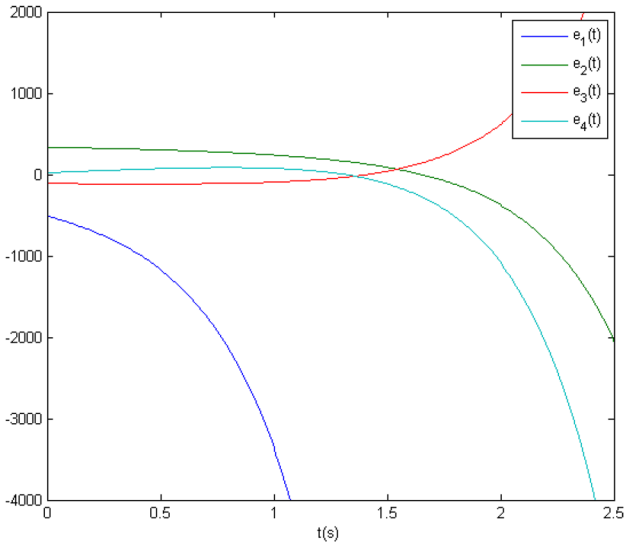

Fig. 3 The trajectories of error system Eq. (7) without control strategy Eq. (9)

4.2 Example 2

Consider a complex network model with two nodes, its drive system is as follows

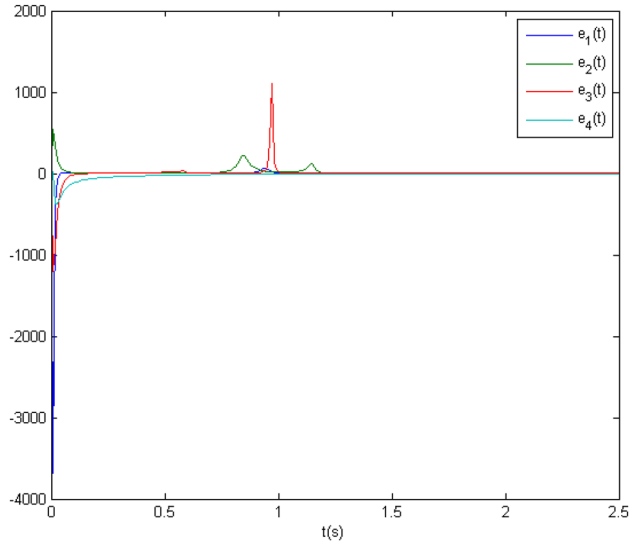

Fig. 4 The trajectories of error system Eq. (7) under control strategy Eq. (9)

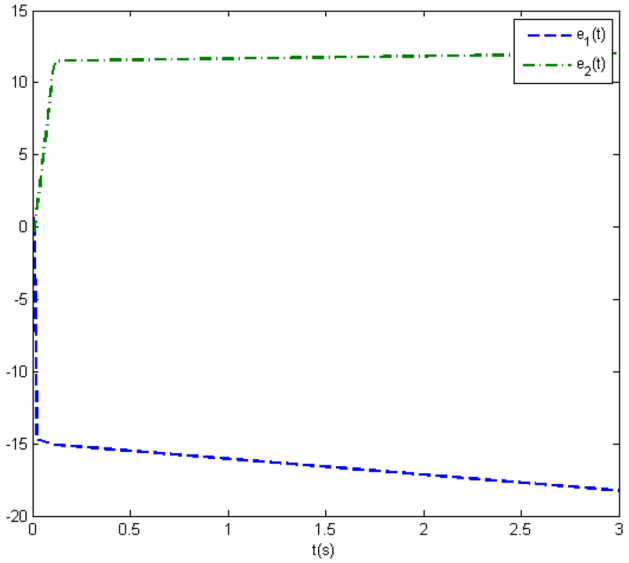

Fig. 5 The synchronization errors between Eqs. (19) and (20) without controller Eq. (24)

$$\begin{aligned}\dot{x}_i(t) &= F(x_i(t)) + f_1(x_i(t-\tau_0(t))) + \sum_{j=1}^{2} b_{ij}^{(1)} h_j(x_j(t)) \\ &+ \sum_{j=1}^{2} l_{ij}^{(1)} h_j(x_j(t-\tau_1(t))) \\ &+ \sum_{j=1}^{2} d_{ij}^{(1)} \int_{t-\tau_2(t)}^{t} h_j(x_j(s))ds \end{aligned} \tag{41}$$

where $F(\cdot) = A(\cdot)\hat{\alpha} + f(\cdot)$, $A(\cdot) = 2 \cdot tanh(x_i(\cdot))$, $f(\cdot) = \tanh(x_i(\cdot))$, $h(\cdot) = 3tanh(x_i(\cdot))$ and take $\hat{\alpha} = (a, b)^T$ as the vector estimates of unknown parameters, where the nominal values are $a = 1.0, b = 5/8$. $f_1(\cdot) = \tanh(x_i(\cdot))$ and

$$\begin{aligned} B^{(1)} &= (b_{ij}^{(1)}) = \begin{pmatrix} \frac{1}{2} & 0 \\ \frac{1}{4} & \frac{1}{2} \end{pmatrix} \\ L^{(1)} &= (l_{ij}^{(1)}) = \begin{pmatrix} 0 & \frac{1}{5} \\ \frac{1}{3} & \frac{1}{2} \end{pmatrix} \\ D^{(1)} &= (d_{ij}^{(1)}) = \begin{pmatrix} \frac{1}{5} & \frac{1}{2} \\ \frac{1}{5} & 0 \end{pmatrix} \end{aligned} \tag{42}$$

The response system is

$$\begin{aligned}\dot{y}_i(t) &= G(y_i(t)) + f_1(y_i(t-\tau_0(t))) \\ &+ \sum_{j=1}^{2} b_{ij}^{(2)} h_j(y_j(t)) + \sum_{j=1}^{2} l_{ij}^{(2)} h_j(y_j(t-\tau_1(t))) \\ &+ \sum_{j=1}^{2} d_{ij}^{(2)} \int_{t-\tau_2(t)}^{t} h_j(y_j(s))ds \end{aligned} \tag{43}$$

where $G(\cdot) = y_i(\cdot)$, $f_1(\cdot) = tanh(y_i(\cdot))$, $h(\cdot) = 3tanh(y_i(\cdot))$,$\tau_0(t) = \tau_1(t) = \tau_2(t) = 0.01 + 0.02\sin(t)$, $\tau_0 = \tau_1 = \tau_2 = 0.03$, $\omega = \bar{\zeta} = \bar{\xi} = 1$, $\mu = 0.05$, $\eta = 3$, $\varrho = 2$. The initial values are $x(t) = (0.3, 2.5)^T$, $y(t) = (0.3, 2.5)^T$ and

$$\begin{aligned} B^{(2)} &= (b_{ij}^{(2)}) = \begin{pmatrix} \frac{1}{5} & 0 \\ \frac{1}{2} & \frac{1}{2} \end{pmatrix} L^{(2)} = (l_{ij}^{(2)}) = \begin{pmatrix} 0 & \frac{1}{2} \\ \frac{1}{6} & \frac{1}{4} \end{pmatrix} \\ D^{(2)} &= (d_{ij}^{(2)}) = \begin{pmatrix} \frac{1}{2} & \frac{1}{5} \\ \frac{1}{2} & 0 \end{pmatrix} \end{aligned} \tag{44}$$

By calculation, $\|\bar{B}\|_1 = 0.75, \|\bar{L}\|_1 = 0.75$, $\|\bar{D}\|_1 = 1, \|B^{(2)} - B^{(1)}\|_\infty = 0.3$, $\|L^{(2)} - L^{(1)}\|_\infty = 0.42, \|D^{(2)} - D^{(1)}\|_\infty = 0.3, t^* \approx 19.97163$, so the conditions of Theorem 2 are satisfied.

The simulations show that the node dynamic behavior can be affected by the controller. Figure 5 shows the motion trajectory of the error uncontrolled system, and it can be seen that the states are not stable. Figure 6 shows the trajectory of the error system under the controller. It is not difficult to see that the 2-dimensional node state error tends to zero and remain steady within t^*, which verifies our theoretical results are effective.

5 Application to Secure Communication

There will be a lot of information transmission in the actual complex network, information security is becoming more and more important. Therefore, secure communication based on complex networks has attracted more and more attention.[33–35] During the encryption process, if there is no decryption key, the document cannot be understood. Secure

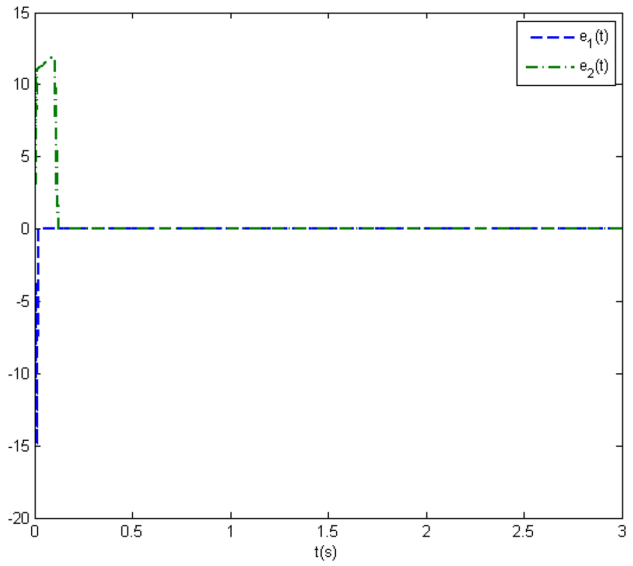

Fig. 6 The synchronization errors between Eqs. (19) and (20) under controller Eq. (24)

communication using synchronization between chaotic systems (referred to as chaotic secure communication) is a new concept of secure communication.[36] Referring to the outer projective synchronization in Sect. 3, it is applied to the secure communication scheme shown in the figure for verification.

The secure communication system shown in Fig. 7 consists of a transmitter system and a receiver system. For easy illustration, the transmitted signal is $m(t) = x(t) + \delta p(t)$. The signal transmitted in the channel is masked by the chaotic signal emitted by the sender to achieve the effect of encryption. Finally, the transmission information is recovered after the chaotic synchronization of the nodes in the network at the receiving end. The transmitter can be described as follows

$$\dot{x_1}(t) = F(x_1(t)) + f_1(x_1(t-\tau_0(t))) + \sum_{j=1}^{2} b_{1j} H_1 x_j(t) + \sum_{j=1}^{2} l_{1j} H_2 x_j(t-\tau_1(t)) + \sum_{j=1}^{2} d_{1j} \int_{t-\tau_2(t)}^{t} H_3 x_j(\xi) d\xi + \delta p(t) \tag{45}$$

$$\dot{x_2}(t) = F(x_2(t)) + f_1(x_2(t-\tau_0(t))) + \sum_{j=1}^{2} b_{2j} H_1 x_j(t) + \sum_{j=1}^{2} l_{2j} H_2 x_j(t-\tau_1(t)) + \sum_{j=1}^{2} d_{2j} \int_{t-\tau_2(t)}^{t} H_3 x_j(\xi) d\xi + 0 \tag{46}$$

where $i, j = 1, 2$. Note that $p(t)$ must consume lower power, that is, be weak in comparison with the chaotic carrier. Therefore we take $\delta = 0.01$.

The receiver can be described as follows

$$\dot{y_1}(t) = G(y_1(t)) + f_1(y_1(t-\tau_0(t))) + \sum_{j=1}^{2} b_{1j} H_1 y_j(t) + \sum_{j=1}^{2} l_{1j} H_2 y_j(t-\tau_1(t)) + u_1(t) - M(t) y_1(t) + \sum_{j=1}^{2} d_{1j} \int_{t-\tau_2(t)}^{t} H_3 y_j(\xi) d\xi + m_1(t) \tag{47}$$

$$\dot{y_2}(t) = G(y_2(t)) + f_1(y_2(t-\tau_0(t))) + \sum_{j=1}^{2} b_{2j} H_1 y_j(t) + \sum_{j=1}^{2} l_{2j} H_2 y_j(t-\tau_1(t)) + u_2(t) - M(t) y_2(t) + \sum_{j=1}^{2} d_{2j} \int_{t-\tau_2(t)}^{t} H_3 y_j(\xi) d\xi + m_2(t) \tag{48}$$

where

$$M(t) = \begin{pmatrix} 4 + \sin(4t) & 0 \\ 0 & 2\sin(3t) \end{pmatrix} \tag{49}$$

$$H_1 = H_2 = H_3 = \begin{pmatrix} 1 & 0 \\ 0 & 1 \end{pmatrix} \quad B = \begin{pmatrix} \frac{1}{5} & 0 \\ \frac{3}{5} & \frac{2}{5} \end{pmatrix} \tag{50}$$

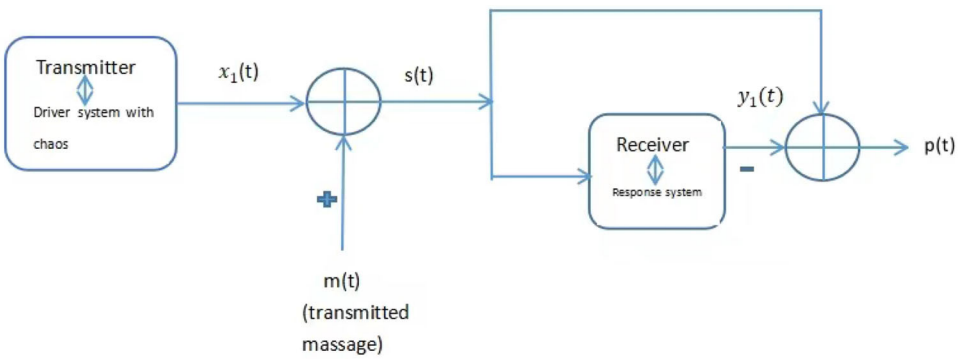

Fig. 7 The presented communication system consisting of a transmitter and a receiver

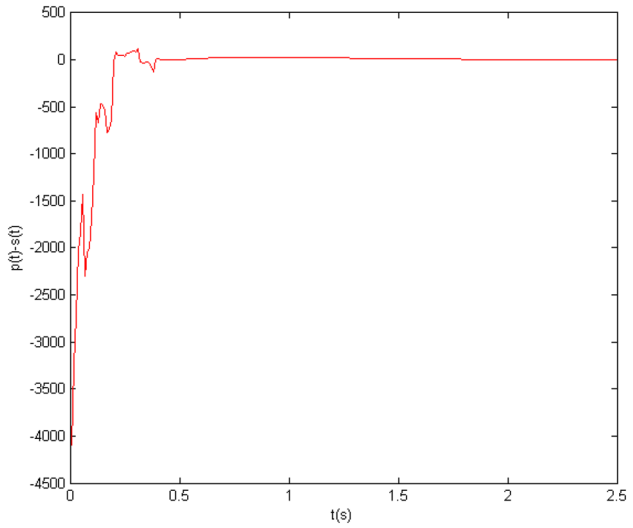

Fig. 8 Output of continuous signal in chaotic masking secure communication system

Similarly, the matrices L,D are expressed as

$$L = \begin{pmatrix} \frac{3}{5} & 0 \\ 0 & \frac{3}{5} \end{pmatrix} \qquad D = \begin{pmatrix} \frac{2}{5} & 0 \\ 0 & \frac{1}{2} \end{pmatrix} \tag{51}$$

and $m_1(t) = x_1(t) + \delta p(t)$, $m_2(t) = x_2(t)$. Where the system parameters are the same as the numerical Example 1 and take the information message as $p(t) = sin(0.001t)$. $m_1(t)$and $m_2(t)$ are the transmitted signal. Due to the fact that the chaotic signal transmitted in the channel is stronger than the transmitted signal, and the latter will be completely covered by the former, it is difficult to be stolen by others by modulating it in the chaotic signal. Driven by $s(t) = \delta^{-1}[m_1(t) - M(t)y_1(t)]$, the chaotic signal at the transmitter and the chaotic signal at the receiver can be approximately synchronized. At the receiver, the signal is extracted by chaotic synchronization as $p(t)$.It can be seen from the Fig. 8 that the error between the transmitted signal and the recovered signal approaches 0 after a period of time. Therefore, the receiver system recovers the transmitted signal quickly and effectively.

6 Conclusions

A class of complex network models with more general and complex structures was constructed and its the outer projection synchronization and finite-time synchronization were studied. A mixed control strategy with adaptive law was presented to realize the outer projective synchronization. A new controller is used to simplify it to solve some difficult finite-time synchronization problems. For different synchronization methods, the conditions for synchronization are given. In real life, there are more complex network models that can be represented by integer-order or even fractional-order systems. Therefore, constructing new and more complex network models and their synchronization problems are our future research topics.

Author Contributions HL: Data, analysis and Writing, Validation, Methodology. NJ: Supervision.

Funding No funding.

Data Availability Editorial Policies for: Springer journals and proceedings: https://www.springer.com/gp/editorial-policies Nature Portfolio journals: https://www.nature.com/nature-research/editorial-policies *Scientific Reports*: https://www.nature.com/srep/journal-policies/editorial-policies BMC journals: https://www.biomedcentral.com/getpublished/editorial-policies

Declarations

Conflict of interest We declare that we do not have any commercial or associative interest that represents a conflict of interest in connection with the work submitted.

References

1. Liu XX et al (2020) Synchronization of complex networks with Markovian switching coupling via aperiodically quantized intermittent pinning control. Asian J Control 23(3):1419–1430
2. El-Saka HAA, Obaya I, Agiza HN (2021) A fractional complex network model for novel corona virus in China. Adv Differ Equ 1:1–19
3. Feng AX et al (2022) Characteristics of vapor based on complex networks in China. Chin Phys B 4:412–426
4. Shafiei M, Parastesh F, Jalili M et al (2019) Effects of partial time delays on synchronization patterns in Izhikevich neuronal networks. Eur Phys J B 92(36):1–7
5. An SH (2020) A review of complex network theory research. Comput Syst Appl 29(9):26–31
6. Ren XL, Meng K (2021) Vector complex network and its application in complex system modeling. Comput Syst Appl 9:309–316
7. Selvaraj P, Sakthivel R, Ahn CK (2019) Observer-based synchronization of complex dynamical networks under actuator saturation and probabilistic faults. IEEE Trans Syst Man Cybern Syst 49(7):1516–1526
8. Zeng HB, Guo LT, He Y, Xu HL, Wang W (2017) Sampled-data synchronization control for chaotic neural networks subject to actuator saturation. Neurocomputing 260:25–31
9. Ali K, Khoshnam S (2020) Synchronization of complex dynamical networks with dynamical behavior links. Asian J Control 22(1):474–485
10. Zhang C, Wang X, Ye X, Zhou S, Feng L (2020) Robust modified function projective lag synchronization between two nonlinear complex networks with different-dimensional nodes and disturbances. ISA Trans 101(6):42–49
11. Zhao LY, Wu QJ, Wang R (2019) Pinning cluster synchronization of coupled nonidentical harmonic oscillators under directed topology. Asian J Control 21(2):1009–1016
12. Zhang L, Peng JK (2020) A new four-wing chaotic system and its unified generalized projective synchronization. Wuhan Univ J Nat Sci 25(3):256–266

13. Xiao FX (2020) An observer-based exponential synchronization scheme for chaotic systems: using advanced encryption standard as auxiliary. Asian J Control 22(6):2183–2205
14. Chen G, Zhao M, Zhou T, Wang BH (2017) Synchronization phenomena on networks, encyclopedia of complexity and systems. Science 5:1–23
15. Liu J, Li LL, Habib M (2020) Complete synchronization of coupled Boolean networks with arbitrary finite delays. Front Inf Technol Electron Eng 2:281–293
16. An K, Lin M, Ouyang J, Zhu WP (2016) Secure Transmission in Cognitive Satellite Terrestrial Networks. IEEE J Sel Areas Commun 34(11):3025–3037
17. Yue DH, Shuang LC, Gong LB (2016) Modified function projective synchronization between two complex networks with known or unknown parameters. J Electron Inf 38(7):1816–1822
18. Zhao HB, Yu QW, Yan SY (2022) Projective synchronization experiment of chaotic systems based on pole placement. Lab Sci 25(02):23–26
19. Zhang C, Wang XY, Wang SB, Zhou WJ, Xia ZQ (2018) Finite-time synchronization for a class of fully complex-valued networks with coupling delay. IEEE Access 6:17923–17932
20. Zhao H, Li L, Peng H et al (2017) Finite-time topology identification and stochastic synchronization of complex networks with multiple time delays. Neurocomputing 219:39–49
21. Feng JW, Li N, Zhao Y, Xu C, Wang JY (2017) Finite-time synchronization analysis for general complex dynamical networks with hybrid couplings and time-varying delays. Nonlinear Dyn 88(4):2723–2733
22. Chen C, Li LX, Peng HP, Yang YX, Li T (2017) Finite-time synchronization of memristor-based neural networks with mixed delays. Neurocomputing 235:83–89
23. Wang G, Lu SW, Liu WB, Ma RN (2021) Adaptive complete synchronization of two complex networks with uncertain parameters, structures, and disturbances. J Comput Sci 54:101436
24. Wu LG, Su XJ et al (2011) A new approach to stability analysis and stabilization of discrete-time T-S fuzzy time-varying delay systems. IEEE Trans Syst Man Cybern Part B 41(1):273–286
25. Gao Y, Qiu TS, Sha L, Zhao YB (2009) Narrowband time delay estimation based on correlation coefficient. J Syst Eng Electron 5:937–941
26. Jia Y, Li GW, Tao JT, He HW, Xiao X (2020) Application of sliding mode predictive control in pure time delay system. Front Inf Technol Electron Eng 2:281–293
27. Du W, Li Y, Zhang J (2022) Stability analysis and control of an extended car following model under honk environment. Int J ITS Res 20:1–10
28. Zhao JX, Shao YF (2021) Effects of time-varying delays on the stability of a class of stochastic competitive system. Math Appl 34(3):674–686
29. Han M, Zhang YM, Zhang M (2016) Modified function projective synchronization between two different complex networks with delayed couplings and delayed nodes of different dimensions. Int J Mod Phys C 27(11):1–17
30. Zhao YP, He P, Nik HS, Ren JC (2015) Robust adaptive synchronization of uncertain complex networks with multiple time-varying coupled delays. Complexity 20(6):62–73
31. Zheng CD, Shan QH, Wei ZP (2018) Stochastic synchronization for an array of hybird neural networks with random coupling strengths and unbounded distributed delays. Neurocomputing 273:22–36
32. Liu Y, Liu M, Xu X (2021) Fixed-time synchronization of stochastic complex networks with Markov jump and mixed delays via adaptive non-chattering control. Optim Control Appl Methods 43:1–15
33. Alimi AM, Aouiti C, Assali E (2019) Finite-time and fixed-time synchronization of a class of inertial neural networks with multi-proportional delays and its application to secure communication. Neurocomputing 332:29–43
34. Wang WP, Jia X, Luo X et al (2019) Fixed-time synchronization control of memristive MAM neural networks with mixed delays and application in chaotic secure communication. Chaos Solitons Fractals 126:85–96
35. An XL, Yu JN, Li YZ, Chu YD, Zhang JG, Li XF (2011) Design of a new multistage chaos synchronized system for secure communications and study on noise perturbation. Math Comput Model 54:7–18
36. Yang T (2004) A survey of chaotic secure communication systems. Int J Comput Cogn 2(2):81–130